Numerical modelling of lanthanide-ion doped fibre lasers operating within mid-infrared wavelength region

Ł. Sójka[1], D. Furniss[1], Z. Tang[1], H. Sakr[1], E. Barney[1], T.M. Benson[1], A.B. Seddon[1], S. Sujecki[1], K. Scholle[2], S. Lamrini[2] and P. Fuhrberg[2]

[1]*George Green Institute for Electromagnetics Research, University of Nottingham, University Park, NG7 2RD Nottingham, UK, Tel: (+44115) 9515550, Fax: (+44115) 9515616, e-mail: Slawomir.Sujecki@notingham.ac.uk*

[2]*LISA laser products OHG Fuhrberg & Teichmann*
Max-Planck-Str. 1 D- 37191 Katlenburg-Lindau Germany

ABSTRACT

We discuss the numerical modelling of lanthanide-ion doped chalcogenide glass fibre lasers for operation in the mid-infrared wavelength region. We extract the modelling parameters from emission and absorption measurements using Judd-Ofelt and McCumber theory. Numerical algorithms are developed based on the experimentally extracted fibre parameters. The simulation results predict lasing with slope efficiency of at least 20 % provided, that the fibre loss can be kept at the level of 1 dB/m or less.

Keywords: fibre laser modelling, mid-infrared light, numerical modelling.

1. INTRODUCTION

Mid-infrared (MIR) coherent light sources are relevant to many potential markets that include medicine, environmental monitoring, pharmaceutical industry, *etc*. Currently available MIR lasers include quantum cascade lasers (QCLs), optical parametric oscillators (OPOs), difference frequency generation (DFG) sources, solid state, fibre and gas lasers. MIR fibre lasers potentially offer good quality of the output beam, large wavelength tuning ability, pulsed operation, relatively large pumping efficiency and contained beam delivery. The longest lasing wavelength that has so far been achieved by a lanthanide ion doped fibre laser is 3.9 μm [1]. A Ho^{3+} doped fluoride (ZBLAN) fibre was used for this purpose and there was a need to apply liquid nitrogen cooling. For many applications liquid nitrogen cooling would impose a severe impediment. Hence, considerable effort has been invested into developing MIR fibre lasers for room temperature operation [2-4]. In 2014 an Er^{3+} ion doped ZBLAN fibre laser was demonstrated, which operates at room temperature at 3.604 μm [3], while in [4] successfully development of a ZBLAN fibre laser with output power in excess of 1 W at 3.44 μm was presented. Further, increase of the ZBLAN fibre laser room temperature operating wavelength is impeded by the relatively high glass matrix maximum phonon energy. Therefore, in order to access longer fibre lasing wavelengths, fibres with a lower maximum phonon energy must be developed. One of the promising candidates for achieving this is the chalcogenide glass family. There is a large body of literature reporting strong MIR photoluminescence (PL), extending up to nearly 6 μm, from lanthanide ion doped chalcogenide glass fibre and bulk samples [5-10]. Chalcogenide fibres are chemically stable, mechanically robust and can attain a low attenuation within the MIR wavelength range [11, 12]. Moreover, Raman lasers based on chalcogenide glass fibres with operating wavelengths up to 3.77 μm have been demonstrated [13, 14]. Finally, recently in [15], chalcogenide fibre has been reported to be successfully thermally spliced with silica fibre thus facilitating the coupling of pump power from a commercially available pig-tailed laser diode [15]. All of these achievements show the potential of the lanthanide ion doped chalcogenide glass fibre technology for the realisation of MIR lasers. The theoretical studies carried out to date show that lanthanide ion doped chalcogenide glass fibre lasers could potentially achieve a wall plug efficiency of up to 20 % when using a cascade pumping scheme [16-18]. Here, we present numerical modelling of alternative pumping schemes for chalcogenide glass lanthanide doped fibre lasers. We studied the properties of a Pr^{3+} doped chalcogenide glass fibre laser that is resonantly pumped using a quantum cascade laser (QCL) and a 3 level lasing system realised by doping selenide based chalcogenide glass with Tb^{3+} ions. Numerical modelling results confirmed the advantages of both pumping schemes when compared with the cascade pumping schemes of [16-18].

2. MODEL DESCRIPTION

For the Tb^{3+} doped glass fibre laser pumped at 2.013 μm or 2.95 μm (Fig.1 and Fig.2, respectively), the energy level populations are obtained from:

$$W_{pa}N_3 - \left(W_{pe} + 1/\tau_{32}\right)N_3 - N_3/\tau_{31} = 0 \qquad (1a)$$

$$W_{sa}N_1 - \left(W_{se} + 1/\tau_{21}\right)N_2 + N_3/\tau_{32} = 0 \qquad (1b)$$

$$N_1 + N_2 + N_3 = N_{Tb} \tag{1c}$$

while for the Pr^{3+} doped glass fibre laser (Fig.3) the energy level populations are calculated by solving:

$$W_{esa} N_2 - (W_{ese} + 1/\tau_{31} + 1/\tau_{32}) N_3 = 0 \tag{2a}$$

$$(W_{sa} + W_{pa}) N_1 - (W_{se} + W_{pe} + 1/\tau_{21} + W_{esa}) N_2 + (W_{ese} + 1/\tau_{32}) N_1 = 0 \tag{2b}$$

$$N_1 + N_2 + N_3 = N_{\mathrm{Pr}} \tag{2c}$$

where N_{Tb} and N_{Pr} is the Tb^{3+} and Pr^{3+} dopant ion concentration, respectively. The symbols τ_i denote level i lifetime. The excited state absorption rate and the stimulated emission rate are calculated from:

$$W_{esa} = \frac{\lambda_p \Gamma_p \sigma_{esa}}{hcA_{eff}} N_2 \left(P_p^+ + P_p^-\right);\ W_{ese} = \frac{\lambda_p \Gamma_p \sigma_{ese}}{hcA_{eff}} N_3 \left(P_p^+ + P_p^-\right) \tag{3a}$$

$$W_{pa} = \frac{\lambda_p \Gamma_p \sigma_{pa}}{hcA_{eff}} N_1 \left(P_p^+ + P_p^-\right);\ W_{pe} = \frac{\lambda_p \Gamma_p \sigma_{pe}}{hcA_{eff}} N_2 \left(P_p^+ + P_p^-\right) \tag{3b}$$

$$W_{sa} = \frac{\lambda_s \Gamma_s \sigma_{sa}}{hcA_{eff}} N_1 \left(P_s^+ + P_s^-\right);\ W_{se} = \frac{\lambda_s \Gamma_s \sigma_{se}}{hcA_{eff}} N_2 \left(P_s^+ + P_s^-\right) \tag{3c}$$

The evolution of the pump and signal powers (P_p and P_s respectively) is described by the equations:

$$\pm \frac{\partial P_p^\pm}{\partial z} = \Gamma_p \left(\sigma_{pe} N_2 - \sigma_{pa} N_1\right) P_p^\pm + \left(\sigma_{ese} N_3 - \sigma_{esa} N_2\right) P_p^\pm - \alpha_p P_p^\pm \tag{4a}$$

$$\pm \frac{\partial P_s^\pm}{\partial z} = \Gamma_s \left(\sigma_{21e} N_2 - \sigma_{21a} N_1\right) P_s^\pm - \alpha_s P_s^\pm \tag{4b}$$

The partial differential equations (4) are solved subject to the following boundary conditions:

$$P_p^+(z=0) = R_p(z=0) P_p^-(z=0) + \left(1 - R_p(z=0)\right) P_{pump} \tag{5a}$$

$$P_p^-(z=L) = R_p(z=L) P_p^+(z=L) \tag{5b}$$

$$P_s^+(z=0) = R_s(z=0) P_s^-(z=0) \tag{5c}$$

$$P_s^-(z=L) = R_s(z=L) P_s^+(z=L) \tag{5d}$$

where L is the cavity length, R_p and R_s are the facet power reflectivity for the pump and signal waves, respectively, while P_{pump} stands for the pump power launched into the fibre at z = 0 (Fig.4). We solved equations (1-4) using the relaxation method (RM) [19] due to its robustness.

3. NUMERICAL RESULTS

In Tables 1-3 we list the modelling parameters. The values of emission and absorption cross sections were obtained from experimental Fourier Transform Infrared (FTIR) spectroscopy measurements of bulk chalcogenide glass samples doped with terbium and praseodymium ions which were prepared in house. The respective emission cross-sections were obtained from the absorption cross-section spectra using McCumber theory and were verified by experimentally measuring PL spectra. The radiative lifetimes were obtained by applying Judd-Ofelt theory to FTIR results and verified by PL lifetime measurements. The excited state absorption spectrum was extracted using McCumber theory from PL spectra measured in [6]. The non-radiative lifetimes resulting from phonon assisted transitions were extracted by fitting the experimental results taken from [6-8].

The modelled example fibre laser structure consisted of a length of a fibre pumped at one side (Fig.4). In the model, fibre gratings trapped the signal and pump light within the fibre cavity. Figure 5 shows the dependence of the MIR signal wave power on the pump power that was calculated using the developed model. These numerical results predicted that when using all three pumping methods an achievement of slope efficiency of at least 20 % is possible.

ACKNOWLEGMENTS

This research has been supported by the European Commission through FP7 Project MINERVA (317803; www.minerva-project.eu): Mid- to NEaR infrared spectroscopy for improved medical diAgnostics and EPSRC pump priming grant RDF/0312: Three level lasing host for mid infrared (MIR) generation.

Table 1. Modelling parameters for Tb^{3+}.

parameter	Unit	value
$\tau_{31}(\lambda_p=2.013\ \mu m)$	ms	0.012
$\tau_{21}(\lambda_p=2.013\ \mu m)$	ms	10.18
$\tau_{32}(\lambda_p=2.013\ \mu m)$	ms	0.0119
$\tau_{31}(\lambda_p=2.95\ \mu m)$	ms	0.012
$\tau_{21}(\lambda_p=2.\ 95\ \mu m)$	ms	10.18
$\tau_{32}(\lambda_p=2.\ 95\ \mu m)$	ms	0.012
$\sigma_{pa}(\lambda_p=2.013\ \mu m)$	m^2	0.73×10^{-24}
$\sigma_{pe}(\lambda_p=2.013\ \mu m)$	m^2	0.7×10^{-24}
$\sigma_{pa}(\lambda_p=2.95\ \mu m)$	m^2	1.03×10^{-24}
$\sigma_{pe}(\lambda_p=2.95\ \mu m)$	m^2	0.53×10^{-24}
σ_{sa}	m^2	1.47×10^{-24}
σ_{se}	m^2	1.00×10^{-24}
λ_s	m	$4.7\text{x}10^{-6}$

Table 2. Modelling parameters for Pr^{3+}.

Parameter	Unit	value
τ_{31}	ms	3.53
τ_{21}	ms	10.1
τ_{32}	ms	8.027
σ_{esa}	m^2	0.306×10^{-24}
σ_{ese}	m^2	0.896×10^{-24}
σ_{pa}	m^2	0.622×10^{-24}
σ_{pe}	m^2	1.711×10^{-24}
σ_{sa}	m^2	0.376×10^{-24}
σ_{se}	m^2	0.849×10^{-24}
λ_p	m	$4.15\text{x}10^{-6}$
λ_s	m	$4.9\text{x}10^{-6}$

Table 3. Fiber laser modelling parameters.

Parameter	Unit	value
N_{Tb} N_{Pr}	$1/\ m^3$	0.825×10^{25} $0.96\text{x}10^{25}$
L	m	1.0
Γ_p		0.9
Γ_s		0.9
α_p	1/m	0.23
α_s	1/m	0.23
$R_p(z=0)$		0.05
$R_p(z=L)$		0.95
$R_s(z=0)$		0.05
$R_s(z=L)$		0.95

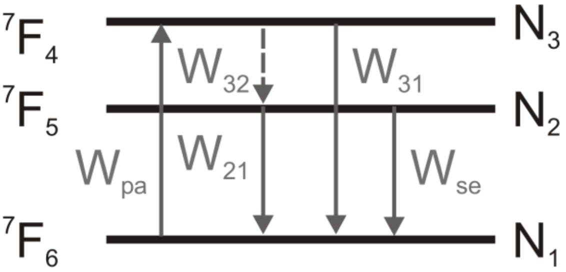

Fig.1. Schematic diagram of energy levels of Tb^{3+} pumped at 2.95 µm.

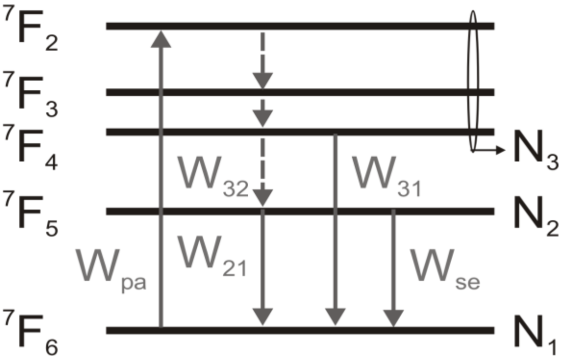

Fig.2. Schematic diagram of energy levels of Tb^{3+} pumped at 2.013 µm.

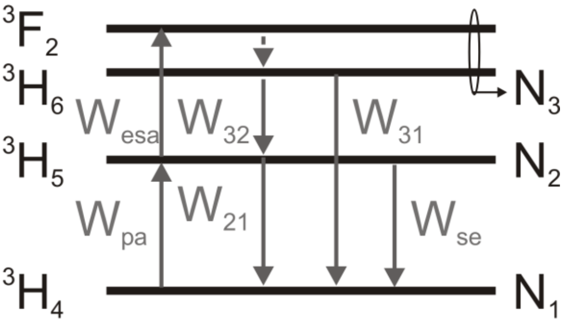

Fig.3. Schematic diagram of energy levels of Pr^{3+} pumped resonantly at 4.15 µm.

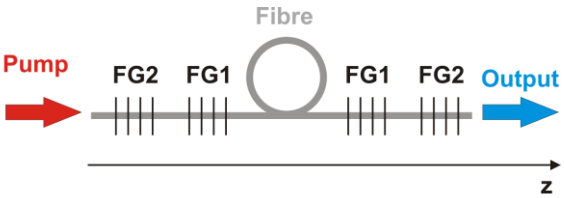

Fig.4. Modelled fibre laser structure; Fibre gratings FG1 and FG2 trap the signal and the pump, respectively, within the cavity.

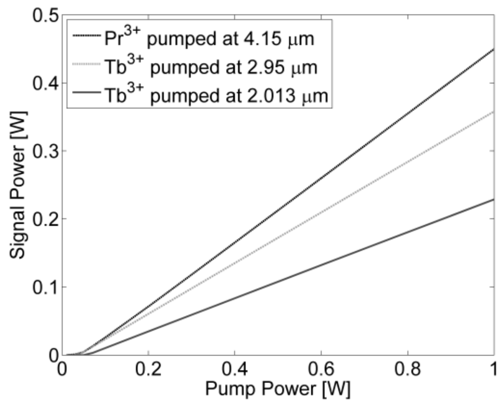

Fig.5. Dependence of the MIR signal power on the pump power for the fibre laser structure from Fig.4.

REFERENCES

[1] J. Schneider, C. Carbonnier, and U. B. Unrau, "Characterization of a Ho^{3+}-doped fluoride fiber laser with a 3.9-μm emission wavelength," Applied Optics **36**, 8595-8600 (1997).

[2] C. Carbonnier, H. Tobben, and U. B. Unrau, "Room temperature CW fibre laser at 3.22 μm," Electronics Letters **34**, 893-894 (1998).

[3] O. Henderson-Sapir, J. Munch, and D. J. Ottaway, "Mid-infrared fiber lasers at and beyond 3.5 μm using dual-wavelength pumping," Optics Letters **39**, 493-496 (2014).

[4] V. Fortin, F. Maes, M. Bernier, S. Tobou Bah, M. D'Auteuil, and R. Vallee, "Watt-level erbium-doped all-fiber laser at 3.44 μm," accepted for publication, Optics Letters (2016).

[5] J. S. Sanghera, L. B. Shaw, and I. D. Aggarwal, "Chalcogenide Glass-Fiber-Based Mid-IR Sources and Applications," Ieee Journal of Selected Topics in Quantum Electronics **15**, 114-119 (2009).

[6] L. B. Shaw, B. Cole, P. A. Thielen, J. S. Sanghera, and I. D. Aggarwal, "Mid-wave IR and long-wave IR laser potential of rare-earth doped chalcogenide glass fiber," IEEE Journal of Quantum Electronics **37**, 1127-1137 (2001).

[7] H. Sakr, D. Furniss, Z. Tang, L. Sojka, N. A. Moneim, E. Barney, S. Sujecki, T. M. Benson, and A. B. Seddon, "Superior photoluminescence (PL) of Pr^{3+}-In, compared to Pr^{3+}-Ga, selenide-chalcogenide bulk glasses and PL of optically-clad fiber," Optics Express **22**, 21236-21252 (2014).

[8] L. Sojka, Z. Tang, D. Furniss, H. Sakr, A. Oladeji, E. Beres-Pawlik, H. Dantanarayana, E. Faber, A. B. Seddon, T. M. Benson, and S. Sujecki, "Broadband, mid-infrared emission from Pr^{3+} doped GeAsGaSe chalcogenide fiber, optically clad," Optical Materials **36**, 1076-1082 (2014).

[9] Z. Tang, D. Furniss, M. Fay, H. Sakr, L. Sojka, N. Neate, N. Weston, S. Sujecki, T. M. Benson, and A. B. Seddon, "Mid-infrared photoluminescence in small-core fiber of praseodymium-ion doped selenide-based chalcogenide glass," Optical Materials Express **5**, 870-886 (2015).

[10] M. F. Churbanov, I. V. Scripachev, V. S. Shiryaev, V. G. Plotnichenko, S. V. Smetanin, E. B. Kryukova, Y. N. Pyrkov, and B. I. Galagan, "Chalcogenide glasses doped with Tb, Dy and Pr ions," Journal of Non-Crystalline Solids **326**, 301-305 (2003).

[11] Z. Tang, V. S. Shiryaev, D. Furniss, L. Sojka, S. Sujecki, T. M. Benson, A. B. Seddon, and M. F. Churbanov, "Low loss Ge-As-Se chalcogenide glass fiber, fabricated using extruded preform, for mid-infrared photonics," Optical Materials Express **5**, 1722-1737 (2015).

[12] G. E. Snopatin, M. F. Churbanov, A. A. Pushkin, V. V. Gerasimenko, E. M. Dianov, and V. G. Plotnichenko, "High purity arsenic-sulfide glasses and fibers with minimum attenuation of 12 dB/km," Optoelectronics and Advanced Materials-Rapid Communications **3**, 669-671 (2009).

[13] M. Bernier, V. Fortin, N. Caron, M. El-Amraoui, Y. Messaddeq, and R. Vallee, "Mid-infrared chalcogenide glass Raman fiber laser," Optics Letters **38**, 127-129 (2013).

[14] M. Bernier, V. Fortin, M. El-Amraoui, Y. Messaddeq, and R. Vallee, "3.77 μm fiber laser based on cascaded Raman gain in a chalcogenide glass fiber," Optics Letters **39**, 2052-2055 (2014).

[15] R. Thapa, R. R. Gattass, V. Nguyen, G. Chin, D. Gibson, W. Kim, L. B. Shaw, and J. S. Sanghera, "Low-loss, robust fusion splicing of silica to chalcogenide fiber for integrated mid-infrared laser technology development," Optics letters **40**, 5074-5077 (2015).

[16] R. S. Quimby, L. B. Shaw, J. S. Sanghera, and I. D. Aggarwal, "Modeling of cascade lasing in Dy : Chalcogenide glass fiber laser with efficient output at 4.5 μm," IEEE Photonics Technology Letters **20**, 123-125 (2008).

[17] L. Sojka, Z. Tang, H. Zhu, E. Beres-Pawlik, D. Furniss, A. B. Seddon, T. M. Benson, and S. Sujecki, "Study of mid-infrared laser action in chalcogenide rare earth doped glass with Dy^{3+}, Pr^{3+} and Tb^{3+}," Optical Materials Express **2**, 1632-1640 (2012).

[18] S. Sujecki, L. Sojka, E. Beres-Pawlik, Z. Tang, D. Furniss, A. B. Seddon, and T. M. Benson, "Modelling of a simple Dy^{3+} doped chalcogenide glass fibre laser for mid-infrared light generation," Optical and Quantum Electronics **42**, 69-79 (2010).

[19] S. Sujecki, "An Efficient Algorithm for Steady State Analysis of Fibre Lasers Operating under Cascade Pumping Scheme," Intl journal of electronics and telecommunications **60**, 143-149 (2014).